Calcium-induced Calcium Release in Smooth Muscle✪

Loose Coupling between the Action Potential and Calcium Release

M.L. Collier, G. Ji, Y.-X. Wang, and M.I. Kotlikoff

From the Department of Animal Biology, School of Veterinary Medicine, University of Pennsylvania, Philadelphia, Pennsylvania 19104-6046

abstract Calcium-induced calcium release (CICR) has been observed in cardiac myocytes as elementary calcium release events (calcium sparks) associated with the opening of L-type Ca^{2+} channels. In heart cells, a tight coupling between the gating of single L-type Ca^{2+} channels and ryanodine receptors (RYRs) underlies calcium release. Here we demonstrate that L-type Ca^{2+} channels activate RYRs to produce CICR in smooth muscle cells in the form of Ca^{2+} sparks and propagated Ca^{2+} waves. However, unlike CICR in cardiac muscle, RYR channel opening is not tightly linked to the gating of L-type Ca^{2+} channels. L-type Ca^{2+} channels can open without triggering Ca^{2+} sparks and triggered Ca^{2+} sparks are often observed after channel closure. CICR is a function of the net flux of Ca^{2+} ions into the cytosol, rather than the single channel amplitude of L-type Ca^{2+} channels. Moreover, unlike CICR in striated muscle, calcium release is completely eliminated by cytosolic calcium buffering. Thus, L-type Ca^{2+} channels are loosely coupled to RYR through an increase in global $[Ca^{2+}]$ due to an increase in the effective distance between L-type Ca^{2+} channels and RYR, resulting in an uncoupling of the obligate relationship that exists in striated muscle between the action potential and calcium release.

key words: calcium-induced calcium release • smooth muscle • Ca^{2+} sparks • excitation–contraction coupling • action potential signaling

INTRODUCTION

In striated muscle excitation–contraction (E-C)[1] coupling is initiated by the gating of sarcolemmal L-type Ca^{2+} channels, which trigger the release of calcium from ryanodine receptors (RYRs) on the sarcoplasmic reticulum (Endo, 1977; Fabiato, 1983; Nabauer et al., 1989; Tanabe et al., 1990; McPherson and Campbell, 1993). While the mechanism of coupling between L-type Ca^{2+} channels and RYRs is different in skeletal and cardiac myocytes, in both cell types local interactions between these proteins underlie calcium release. In skeletal myocytes, calcium entry is not required for calcium release (Armstrong et al., 1972), but gating of the L-type Ca^{2+} channel appears to be physically coupled to RYR opening (Tanabe et al., 1990; Nakai et al., 1998). Calcium entry through L-type Ca^{2+} channels triggers calcium-induced calcium release (CICR) in heart cells (Fabiato, 1985; Nabauer et al., 1989), resulting in localized calcium release, termed Ca^{2+} sparks (Cheng et al., 1993; Cannell et al., 1995; Lopez-Lopez et al., 1995). This coupling process involves a local increase in $[Ca^{2+}]_i$ in the microdomain of the L-type Ca^{2+} channel, which is sensed by the RYR, resulting in RYR gating, and several lines of evidence indicate that the opening of a single L-type Ca^{2+} channel triggers a Ca^{2+} spark in an obligatory fashion (Niggli and Lederer, 1990; Cannell et al., 1995; Lopez-Lopez et al., 1995; Santana et al., 1996; Lipp and Niggli, 1996; Collier et al., 1999). This tight coupling between gating of the voltage-dependent sarcolemmal channel and the sarcoplasmic reticular release channel underlies the full mobilization of Ca^{2+} that occurs in cardiac myocytes with each action potential.

RYRs are widely expressed in nonsarcomeric (smooth) muscle, neurons, and nonexcitable cells, although their role in calcium release and cellular signaling is poorly understood. In smooth muscle, RYRs are expressed on the sarcoplasmic reticulum (Carrington et al., 1995; Lesh et al., 1998) and triggered Ca^{2+} release has been inferred from measurements of calcium-activated membrane currents and spatially averaged $[Ca^{2+}]_i$ (Zholos et al., 1992; Ganitkevich and Isenberg, 1992, 1995), but little direct evidence of CICR exists and the function of RYRs in E-C coupling is poorly understood. Spontaneous Ca^{2+} sparks have been reported in smooth muscle (Nelson et al., 1995; Mironneau et al., 1996; Gordienko et al., 1998), and recent experiments combining confocal microscopy and patch-clamp techniques have demonstrated localized calcium release during depolarizing voltage-clamp steps (Arnaudeau et al., 1997; Imaizumi et al., 1998), further supporting the existence of CICR in smooth muscle. Here we show that the L-type Ca^{2+}

Address correspondence to Michael I. Kotlikoff, Department of Animal Biology, University of Pennsylvania, 3800 Spruce Street, Philadelphia, PA 19104-6046. Fax: 215-573-6810; E-mail: mik@vet.upenn.edu

✪The online version of this article contains supplemental material.

[1]*Abbreviations used in this paper:* CICR, calcium-induced calcium release; E-C, excitation–contraction; RYR, ryanodine receptor; SR, sarcoplasmic reticulum.

J. Gen. Physiol. © The Rockefeller University Press • 0022-1295/2000/05/653/10 $5.00
Volume 115 May 2000 653–662
http://www.jgp.org/cgi/content/full/115/5/653

current (I_{Ca}) evokes CICR in single urinary bladder myocytes and establish the relationship between L-type Ca^{2+} channel opening and RYR-mediated calcium release in smooth muscle.

MATERIALS AND METHODS

Cell Isolation

Male New Zealand White rabbits were anesthetized (50 mg/kg ketamine, 5 mg/kg xylazine IM) and killed (100 mg/kg pentobarbital i.v.) in accordance with an approved laboratory animal protocol. The urinary bladder was removed, dissected in ice-cold oxygenated physiological salt solution, minced, and suspended in modified collagenase type II (Worthington Biochemical), 1 mg/ml protease type XIV and 5 mg/ml bovine serum albumin (Sigma-Aldrich) at 37°C for 35–40 min. Digested tissue was triturated with a wide-bore Pasteur pipette and passed through a 125-μm nylon mesh; cells were concentrated by low speed centrifugation, washed with fresh medium, resuspended, and stored at 4°C.

Electrophysiology

Single myocytes were placed in a chamber mounted on an inverted Nikon TE300 microscope (Nikon) and whole-cell recordings made as previously described (Wang and Kotlikoff, 1997). In most experiments, pipettes were filled with (mM): 127 cesium glutamate, 10 HEPES (cesium-salt), 19 TEACl, 0.1 Tris-GTP, 1 Mg-ATP, 5 $Tris_2$-creatine phosphate, and 0.1 fluo-4 (pentapotassium salt) at pH 7.2. Heparin (2–5 mg/ml) was added to the internal solution in some experiments. In experiments where the buffering capacity of the internal solution was increased, pipettes were filled with (mM): 110 CsCl, 5 HEPES (cesium-salt), 17 EGTA, 0.1 Tris-GTP, 1 Mg-ATP, 5 $Tris_2$-creatine phosphate, and 3 fluo-4 (pentapotassium salt), with intracellular Ca^{2+} concentration adjusted to 100 nM at pH 7.2. The external solution contained (mM): 137 NaCl, 5 CsCl, 2 $CaCl_2$, 1 NaH_2PO_4, 1.2 $MgCl_2$, 10 HEPES, and 5 glucose at pH 7.4. Caffeine (10 mM) was applied to cells using a picospritzer (General Valve Corp.). Voltage-pulse protocols and the resulting membrane currents were acquired and analyzed using pCLAMP software (Axon Instruments, Inc.). Difference current was obtained either by linear leak subtraction or by blocking L-type Ca^{2+} current by substituting $CaCl_2$ with 500 μM $CdCl_2$. In experiments using ryanodine, cells were pre-incubated with the drug for 1 h at room temperature and 10 μM ryanodine was added to the bath solution.

Cells were field stimulated using a Grass S88 pulse stimulator (Grass Medical Instruments) connected to platinum wires placed in the recording chamber. The stimulus amplitude and duration were 70 V and 10 ms, respectively. Cells were incubated with 10 μM fluo-4 methoxymethylester (Molecular Probes, Inc.) and 0.02% pluronic acid in the dark for 20 min at room temperature, washed with fresh medium, and allowed to de-esterify for 40 min.

Recording and Measurement of Fluorescence

Fluo-4 fluorescence was excited with 488 nm light emitted from a Krypton/Argon laser and measured with a high speed laser scanning confocal head (Noran Oz), using a plan-apo, 60× water-immersion objective lens (1.2 NA; Nikon) and Intervision software on an Indy workstation (Silicon Graphics Inc.). x–y images were collected every 8.3 ms (256 × 240 pixels), and x–t images were obtained with line scans at 4.16-ms intervals for 2.13 s (512 × 480 pixels). Pixel size in the x axis was equal to 0.252 μm and in the y axis to 0.248 μm. To synchronize current and fluorescence measurements, a light emitting diode was placed in the path of the photomultiplier detector and switched on for 2 ms, 10 ms before the start of the voltage step. Images were analyzed using either Intervision software (Silicon Graphics Inc.) or a custom written analysis program using Interactive Data Language software (Research Systems Inc.), kindly provided by Drs. Mark Nelson and Adrian Bonev (Dept. of Pharamacology, University of Vermont, Burlington, VT). In all x–y images, a mean background fluorescence value was determined and subtracted from each pixel, and the images were smoothed using a 3 × 3 pixel median filter. Mean baseline fluorescence intensity (F_o) of a cell was obtained by averaging the first six to eight images that did not exhibit transient rises in intracellular Ca^{2+}. Profiles of line-scan images were obtained over a 1-μm region and F_o was obtained by averaging the fluorescence of 30 pixels before a depolarizing step. Ratios of images (F/F_o) and profiles were constructed to reflect changes in fluorescence intensity over time. The previously described pseudo-ratio equation (Cheng et al., 1993) was used to estimate $[Ca^{2+}]_i$, using a K_d value for fluo-4 of 345 nM and assuming basal $[Ca^{2+}]_i$ to be 100 nM. The Ca^{2+} spark criteria were a localized increase in fluorescence (F/F_o) ≥ 1.5, occurring in 20–30 ms, with a decay time of 50–80 ms. Ca^{2+} spark latencies were calculated as the time from the start of the voltage pulse to the point at which the fluorescence exceeded 5% of F_o, and were calculated for Ca^{2+} sparks occurring within the first voltage-clamp step of an experiment, so as not to bias results by an increase in $[Ca^{2+}]_i$ resulting from preceding voltage-clamp steps. Ca^{2+} spark probability was calculated in the following manner. Voltage-clamp steps were analyzed to determine whether or not a Ca^{2+} spark occurred during a specific clamp step. Currents associated with each step were integrated to determine net Ca^{2+} flux, the fluxes were binned, and the probability was calculated by dividing the number of experiments in which a Ca^{2+} spark was evoked by the total number of experiments in the bin. Thus, the probability of a Ca^{2+} spark occurring in voltage-clamp steps after clamp steps in which no Ca^{2+} spark occurred is likely somewhat higher due to the accumulation of Ca^{2+} from previous steps. These probabilities were fit to a Boltzmann equation of the form:

$$P = 1 + \frac{1}{e^{(J_{50}-J)/k}},$$

where J is the Ca^{2+} flux, J_{50} is the flux at which there is a 50% probability of evoking a Ca^{2+} spark, and k is the slope factor of the relationship. All statistical data are presented as mean ± SEM.

Online Supplemental Material

A movie depicting the entire experiment shown in Fig. 1 A is provided. The movie was constructed by superimposing the current and voltage traces up to the end of each image on the confocal images acquired at an interval of 8.3 ms; the contrast of the unratioed grey scale confocal images was adjusted to maximize the range between background and peak fluorescence (Adobe Photoshop). The stacked TIF files were converted to lower resolution JPG files and exported as a movie at 24 fps (Adobe Premier). Higher resolution, ratioed images at the beginning, middle, and end of this movie are shown in Fig. 1 A. This video can be found at http://www.jgp.org/cgi/content/full/115/5/653/DC1.

RESULTS

The L-type Ca^{2+} Channel Current Triggers CICR

Depolarizing voltage-clamp steps activating I_{Ca} in single urinary bladder myocytes triggered one or several Ca^{2+} sparks and subsequent propagated Ca^{2+} waves (Fig. 1). Images acquired at 8.3-ms intervals showed that release began as elementary events at one or several foci, as

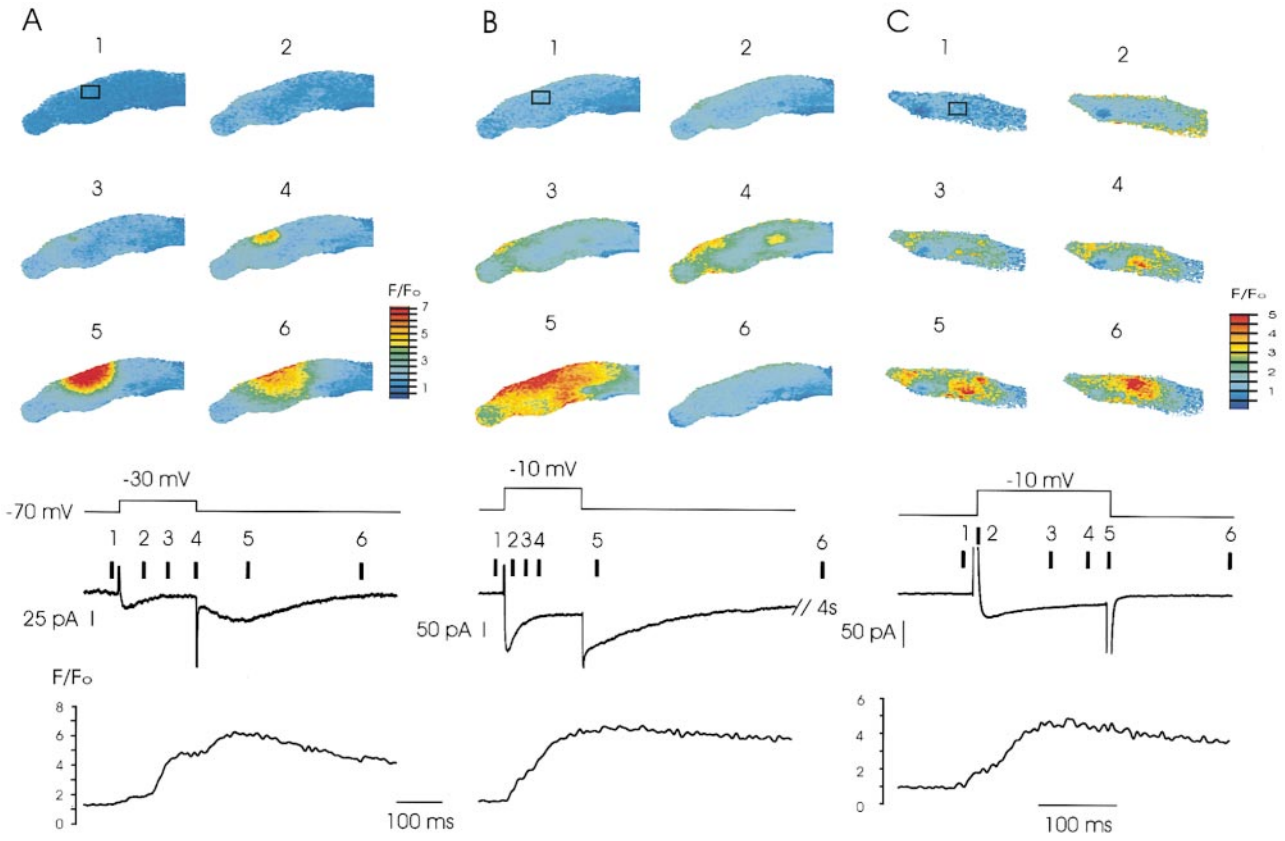

Figure 1. Ryanodine receptors mediate calcium-induced calcium release and Ca^{2+} wave propagation in single urinary bladder myocytes. (Top) Selected x–y confocal images showing Ca^{2+} sparks and propagated Ca^{2+} waves from a series of images acquired every 8.3 ms after step depolarization of a fluo-4–loaded, voltage-clamped bladder myocyte to activate I_{Ca}. Relative fluorescence intensities are indicated by the color bar. (Bottom) Simultaneously recorded relative fluorescence profile from images as shown above and membrane current during a step depolarization to −30 mV (A) and to −10 mV (B and C). The slow tail current after Ca^{2+} release reflects activation of the Ca^{2+}-sensitive chloride current. Numbers correspond to individual images shown at top. (C) The cell was dialyzed with 2 mg/ml heparin. The profile was obtained by averaging pixels within a 10 × 10 pixel (2.52 × 2.48 μm) box (outlined in the first image, top), placed over the area of Ca^{2+} spark initiation. Note that the change in relative fluorescence is delayed at −30 mV compared with that at −10 mV. A movie of Fig. 1 A showing images and current at 8.3 ms intervals is available at http://www.jgp.org/cgi/content/full/115/5/653/DC1.

previously reported (Imaizumi et al., 1998), and progressively expanded to propagated Ca^{2+} waves. The velocity of propagation of the Ca^{2+} wave was 94 ± 15 μm/s (n = 4), similar to Ca^{2+} wave velocity described in cardiac myocytes (Wussling et al., 1997), but substantially faster than Ca^{2+} waves propagated by $InsP_3$ receptors in vascular cells (Bezprozvanny, 1994).

Depolarizations activating smaller currents usually triggered a single Ca^{2+} spark and propagated Ca^{2+} wave, whereas larger currents initiated Ca^{2+} sparks from several sites that propagated and fused. The temporal relationship between I_{Ca} and Ca^{2+} sparks varied with the magnitude of the current, but Ca^{2+} sparks always occurred with a delay after current activation. In some cases, Ca^{2+} sparks were observed only after I_{Ca} was almost completely inactivated (Fig. 1 A). In separate experiments, Ca^{2+} sparks and Ca^{2+} waves were not altered by the dialysis of heparin (Fig. 1 C; n = 4), but were abolished by application of caffeine (10 mM; see Fig. 3; n = 9), incubation with ryanodine (10 μM; see Fig. 5; n = 11), or block of I_{Ca} with $CdCl_2$ (500 μM; not shown; n = 9). The magnitude and kinetics of Ca^{2+} sparks triggered by I_{Ca} was similar to previously reported values for spontaneous Ca^{2+} sparks in smooth muscle. The mean rise time of triggered release events was 26.6 ± 1.6 ms, peak F/F_o = 1.9 ± 0.1, and the half time of decay of isolated (nonpropagated) Ca^{2+} sparks was 62 ± 16 ms (n = 5), which is similar to previous reports using similar methods (Perez et al., 1999). Thus, Ca^{2+} sparks and subsequent Ca^{2+} wave propagation triggered by the voltage-dependent calcium current is due to activation of RYRs by L-type Ca^{2+} channels.

Relationship between I_{Ca} and CICR: Loose Coupling

The number of Ca^{2+} sparks triggered by I_{Ca} and the latency between the onset of the current and the appearance of Ca^{2+} sparks is in sharp contrast to CICR ob-

served in heart cells, in which the latency of the release events (Wier et al., 1994; Cannell et al., 1995; Lopez-Lopez et al., 1995; Collier et al., 1999) closely follows the gating properties of individual L-type Ca^{2+} channels. The small number of Ca^{2+} spark sites evoked by I_{Ca} and the delay between L-type Ca^{2+} channel and RYR channel opening suggested a fundamentally different coupling process in smooth muscle. We hypothesized that, rather than sensing the local elevation of $[Ca^{2+}]_i$ in the vicinity of the Ca^{2+} channel, smooth muscle RYRs were not sensitive to the opening of individual channels, but required a global rise in $[Ca^{2+}]_i$. To test this hypothesis, we first sought to determine whether activation of Ca^{2+} channels always lead to initiation of a Ca^{2+} spark.

As shown in Fig. 2, depolarizing voltage-clamp steps of short duration that initiated a calcium current, but little net calcium flux (JCa^{2+}), did not trigger Ca^{2+} sparks. When the duration of I_{Ca} was progressively increased, Ca^{2+} sparks were observed that occurred well after termination of the depolarizing step and did not propagate. Further lengthening the duration of I_{Ca} resulted in Ca^{2+} sparks that occurred closer to the period of current flow and finally in Ca^{2+} wave propagation. Activation of I_{Ca} without Ca^{2+} release does not occur in cardiac myocytes; rather, evidence suggests that the opening of a single L-type Ca^{2+} channel activates a Ca^{2+} spark (Santana et al., 1996; Collier et al., 1999). This observation and the demonstration of triggered Ca^{2+} sparks after current cessation indicate that L-type Ca^{2+} channels are loosely coupled to RYR channels. That is, L-type Ca^{2+} channels can open without initiating Ca^{2+} sparks in smooth muscle, and the probability of Ca^{2+} sparks occurring after activation of I_{Ca} is a function of current duration and magnitude (see below). It is unlikely that Ca^{2+} sparks during short I_{Ca} were missed and that late-occurring Ca^{2+} sparks were spontaneous events unrelated to I_{Ca} since: (a) measurements were made in line-scan mode using an extended slit width (z resolution at half max = 2.5 μM) to minimize the possibility of missed events; (b) spontaneous events were uncommon in the absence of I_{Ca}, but were always observed if JCa^{2+} was sufficient; (c) the latency of late Ca^{2+} sparks decreased as JCa^{2+} increased (Fig. 2); and (d) propagated Ca^{2+} waves, which were never observed spontaneously, often occurred after the termination of I_{Ca}.

CICR Is a Function of the Magnitude of Ca^{2+} Influx, Not the Amplitude of I_{Ca}

As a further test of whether CICR in smooth muscle requires an increase in global $[Ca^{2+}]_i$ or results from the local response of RYR to the opening of single L-type Ca^{2+} channels, we designed experiments to maximize JCa^{2+} under conditions of low single-channel amplitude, and conversely to maximize the single channel current amplitude under conditions in which JCa^{2+} is low. As shown in Fig. 3 A, bladder myocytes were depolarized to

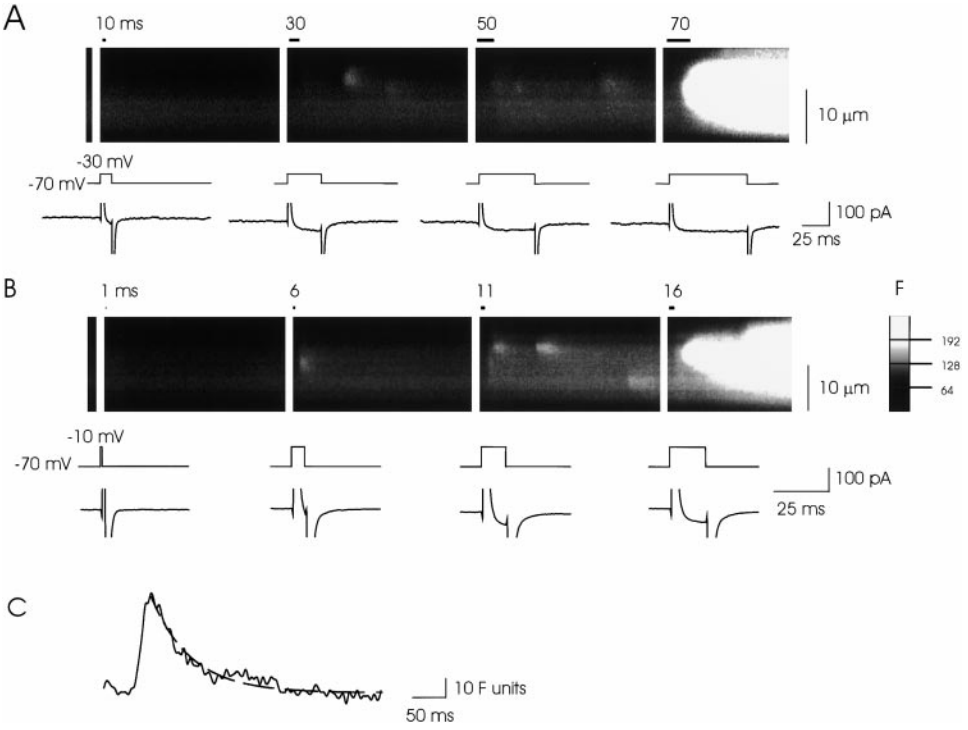

Figure 2. Evoked Ca^{2+} sparks and Ca^{2+} wave propagation depends on the magnitude and duration of I_{Ca}. Short clamp steps do not produce Ca^{2+} sparks, whereas lengthening the current duration results first in delayed Ca^{2+} sparks and then in Ca^{2+} wave propagation. (Top) Confocal line-scan images from a myocyte scanned along a single line at 4.16-ms intervals. The horizontal bar above each line-scan image indicates the period of the depolarizing pulse to −30 mV (A) or to −10 mV (B). The vertical bar indicates the diode flash used to synchronize optical and electrical data. (Bottom) The currents and voltage protocol are shown for each line-scan image in an expanded time scale. Note activation of Ca^{2+} sparks after termination of the depolarizing pulse. (C) The time course of a single Ca^{2+} spark (from 30-ms clamp step in A). The broken line shows a single exponential fit to the Ca^{2+} spark decay; τ = 59 ms.

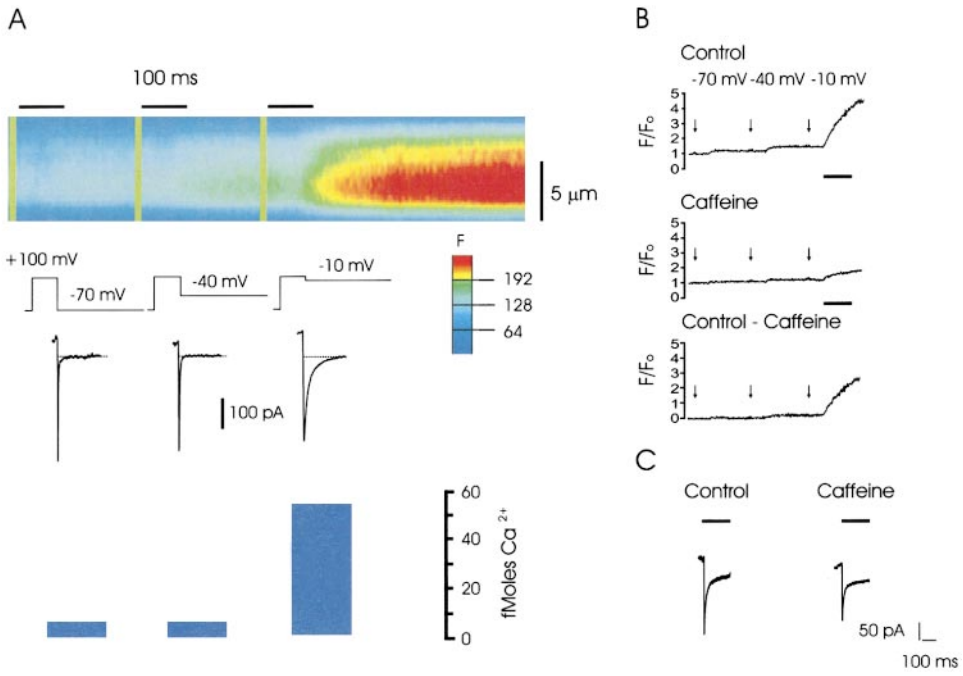

Figure 3. Ca^{2+} sparks and Ca^{2+} wave propagation are specified by the net flux of Ca^{2+}, not the amplitude of I_{Ca}. (A, top) Line-scan image obtained during tail-current protocol. Depolarization (100 mV) period is indicated by the horizontal line, diode flash by the vertical line. (Middle) Voltage protocol and tail currents in time register with scan. (Bottom) Magnitude of Ca^{2+} flux (JCa^{2+}) during each repolarizing pulse. A propagated Ca^{2+} wave is triggered with maximum JCa^{2+} and minimum I_{Ca} amplitude. (B) Fluorescence profile measured over a 1-μm area from line-scan images recorded as in A under control conditions and after exposure to caffeine (10 mM). Difference profile indicates the magnitude of Ca^{2+} release upon repolarization to −10 mV. Arrows indicate the point of repolarization. (C) I_{Ca} tail currents during repolarization to −10 mV before and during caffeine corresponding to the arrows in B.

100 mV for 100 ms to open L-type Ca^{2+} channels (without Ca^{2+} ion permeation), and then to varied potentials to systematically alter the magnitude and duration of the Ca^{2+} tail current. At more negative voltages (−70 mV) the magnitude of the instantaneous current (and the underlying single channel events) is relatively large (∼0.3 pA; Rubart et al., 1996), but the current deactivation is rapid, resulting in little JCa^{2+}. Ca^{2+} sparks were never observed at clamp steps to −70 mV, indicating that brief channel openings of relatively large single channel amplitude do not trigger Ca^{2+} sparks. Conversely, when cells were stepped to −10 mV, where the single channel current amplitude is approximately threefold lower, but JCa^{2+} is much larger due to a longer mean channel open time, CICR was routinely observed ($n = 6$). Thus, smooth muscle RYRs do not sense $[Ca^{2+}]_i$ in the microdomain of the L-type Ca^{2+} channel, since large single channel events (which produce the highest local $[Ca^{2+}]_i$) do not evoke CICR in the absence of sufficient JCa^{2+}. Rather, CICR occurs at low single channel amplitude if the net JCa^{2+} is sufficient. Moreover, the JCa^{2+} requirements for propagated Ca^{2+} waves are incrementally greater than that required to achieve discrete Ca^{2+} sparks. The estimated global $[Ca^{2+}]_i$ achieved immediately before spark propagation was ∼230 nM ($F/F_o = 1.33 \pm 0.09$, $n = 8$). After depletion of sarcoplasmic reticulum (SR) Ca^{2+} stores with caffeine (10 mM), tail current protocols did not result in Ca^{2+} sparks or propagated Ca^{2+} waves. As shown in Fig. 3 B, profiles from line-scan experiments obtained before and after caffeine exposure indicated that after SR depletion the tail protocol resulted in only a small rise in $[Ca^{2+}]_i$, relative to that observed in control steps, despite the fact the equivalent I_{Ca} obtained in both conditions (Fig. 3 C). In the experiment shown, the initial repolarization to −10 mV resulted in a rapid increase in local $[Ca^{2+}]_i$ to greater than threefold baseline, whereas after caffeine application the increase was much smaller and slower.

The relationship between JCa^{2+} and Ca^{2+} spark probability was examined quantitatively in voltage-clamp experiments. JCa^{2+} was calculated from the integrated I_{Ca} in experiments such as that shown in Fig. 2, and the probability of a given JCa^{2+} evoking a Ca^{2+} spark was determined. As shown in Fig. 4 A, the probability of an evoked Ca^{2+} spark increased sharply with JCa^{2+}. Fitting a generalized Boltzmann equation to the data, we determined that the flux at which the probability of evoking a Ca^{2+} spark was 50% occurred with a JCa^{2+} of 4.0 fmol of Ca^{2+}. We also examined the latency to Ca^{2+} spark in experiments at −30 and −10 mV (Fig. 4 B). Latencies were 32.0 ± 13.5 ($n = 5$) and 12.5 ± 2.7 ($n = 10$) in steps to −30 and −10 mV, respectively, significantly longer than observed in cardiac myocytes (<2 ms; Cannell et al., 1995). The voltage dependence of the latency is also consistent with a coupling mechanism related to net Ca^{2+} flux. That is, since the integral of I_{Ca} (and thus the flux of Ca^{2+} ions) increases more rapidly with time at −10 mV than at −30 mV (due

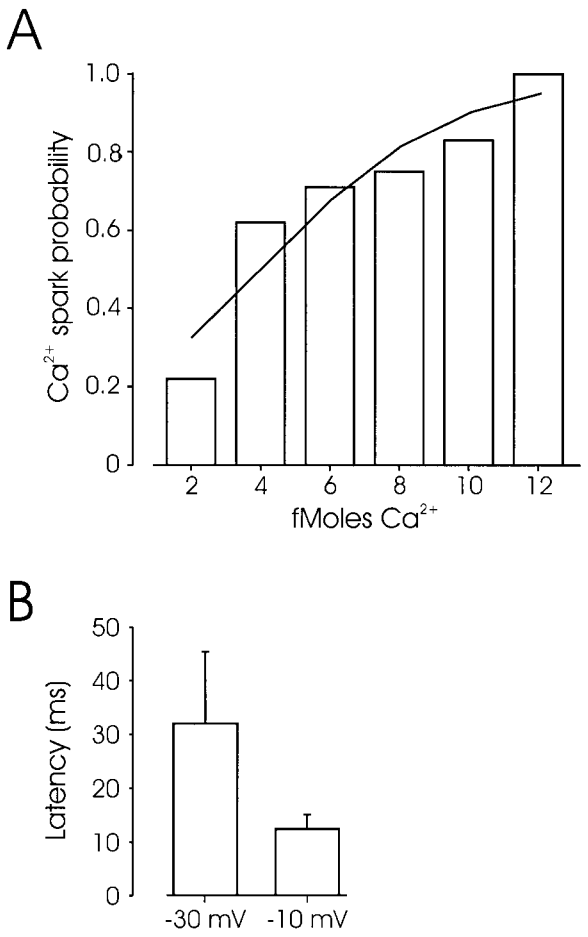

Figure 4. Activation of a Ca^{2+} spark is dependent upon Ca^{2+} flux. (A) The relationship between the probability of Ca^{2+} spark occurrence and the Ca^{2+} flux in the associated current is shown. I_{Ca} from voltage-clamp steps was integrated and binned, and the probability of a Ca^{2+} spark occurring in each bin was determined. The solid line is a fit of the data to a generalized Boltzmann equation with parameters of 50% probability at 4.0 fmol of calcium, and a slope of 2.7. (B) Latencies for Ca^{2+} sparks obtained in voltage-clamp steps to −30 or −10 mV. The latency to Ca^{2+} spark after activation of I_{Ca} was determined from the first voltage-clamp step in experiments similar to Fig. 2; depolarization durations were 6 and 30 ms for voltage-clamp steps to −10 and −30 mV, respectively. Latencies were 32.0 ± 13.5 (n = 5) and 12.5 ± 2.7 (n = 10) at membrane potentials of −30 and −10 mV, respectively.

mainly to the faster rate of current activation at −10 mV), the same Ca^{2+} flux is achieved in shorter time.

Uncoupling of CICR by Chelation of Cytosolic Ca^{2+}

Loose coupling between L-type Ca^{2+} channels and RYR could result from an increase in the effective distance between these proteins, or could indicate a decreased affinity of the ryanodine receptor for Ca^{2+} ions. The spatial separation between a single L-type Ca^{2+} channel and RYR in cardiac cells has been estimated to be <100 nm, based on the fact that high concentrations of mobile Ca^{2+} buffers such as EGTA do not disrupt CICR (Collier and Berlin, 1999), using models of radial diffusion of Ca^{2+} in a concentric shell (Klingauf and Neher, 1997). To examine the effective distance between L-type Ca^{2+} channels and RYR, we sought to determine whether CICR is disrupted in smooth muscle cells in the presence of high concentrations of EGTA, and compared this result with experiments in heart cells recorded under identical conditions. As shown in Fig. 5, CICR was completely eliminated in smooth muscle cells dialyzed with 17 mM EGTA and 3 mM Fluo 4 ($[Ca^{2+}]_i$ clamped at 100 nM; n = 6), whereas CICR was not affected in rat heart cells in equivalent protocols. Thus, Ca^{2+} ions entering through L-type Ca^{2+} channels at a distance >100 nm from RYRs are required for CICR in smooth muscle. We further investigated whether RYR are able to sense local Ca^{2+} entry by performing experiments in which we clamped $[Ca^{2+}]_i$ at 250 and 500 nM, still maintaining 20 mM mobile Ca^{2+} buffer. We reasoned that under conditions of increased global $[Ca^{2+}]_i$, CICR might be triggered by a small additional increase in Ca^{2+} from near (<100 nm) L-type Ca^{2+} channels. However, CICR was not triggered in these experiments, suggesting that the functional distance between the L-type Ca^{2+} channel and RYR is substantially greater than in sarcomeric muscle, despite light microscopic evidence of a close association between calcium channels and RYRs in bladder smooth muscle (Carrington et al., 1995).

Link between Action Potential Discharge and CICR

To determine the relationship between action potential discharge and CICR under relatively physiological conditions, we examined CICR in fluo-4AM–loaded myocytes stimulated at varying frequencies. Rapid acquisition of confocal images during depolarizing stimuli indicated that Ca^{2+} release does not occur with each depolarization (Fig. 6). Rather, local Ca^{2+} sparks and propagated Ca^{2+} waves depend on action potential frequency, revealing complex signal integration at the level of calcium release. Thus, at low stimulation frequencies (0.5 Hz), nonpropagated Ca^{2+} sparks were observed only after accumulation of sufficient depolarizing stimuli (n = 4), and CICR took the form of discrete Ca^{2+} sparks. At higher frequency stimulation (10 Hz), similar to the frequency of spontaneous action potentials reported in guinea-pig bladder myocytes (Klockner and Isenberg, 1985), Ca^{2+} sparks were propagated as Ca^{2+} waves and were repeatedly triggered, often from the same Ca^{2+} release site (n = 6). The frequency of initiation of the propagated Ca^{2+} waves was substantially lower than the stimulation frequency, resulting in an effective low-pass filter of high-frequency electrical signals.

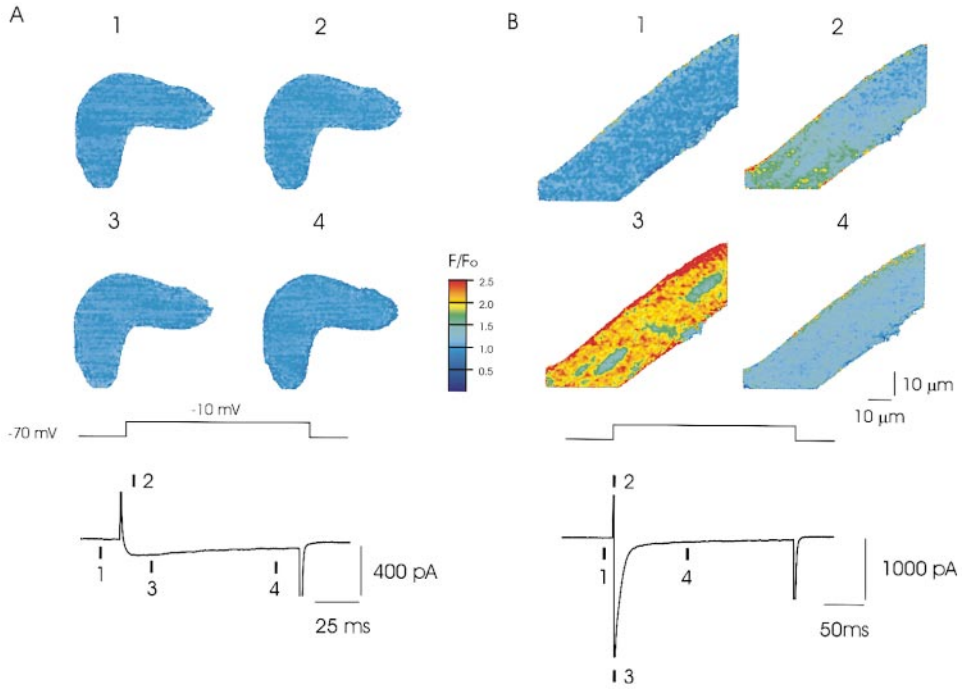

Figure 5. Increased effective distance between L-type Ca^{2+} channels and ryanodine receptors in smooth muscle relative to cardiac muscle. Under conditions of high calcium buffering capacity, I_{Ca} fails to induce Ca^{2+} sparks in smooth muscle cells, whereas Ca^{2+} sparks are abundant in ventricular myocytes. (Top) Confocal x–y images from a series obtained at 8.3-ms intervals from smooth muscle (rabbit urinary bladder, A) and cardiac muscle (rat ventricle, B) cells dialyzed with 17 mM EGTA and 3 mM fluo-4. The scale bars are the same for A and B. (Bottom) Voltage-clamp protocol and corresponding Cd^{2+}-sensitive membrane currents; numbered bars indicate time of corresponding images above.

DISCUSSION

In sarcomeric myocytes, tight coupling exists between gating of the L-type Ca^{2+} channel and RYR such that essentially every L-type Ca^{2+} channel gating event results in the opening of one or more RYR. This coupling derives either from a physical interaction between the proteins in skeletal myocytes (Tanabe et al., 1990; Nakai et al., 1998), or in cardiac myocytes from an interaction between the Ca^{2+} ions permeating the L-type Ca^{2+} channel and subsequently gating RYR. The latter coupling process appears to involve a local sensing of per-

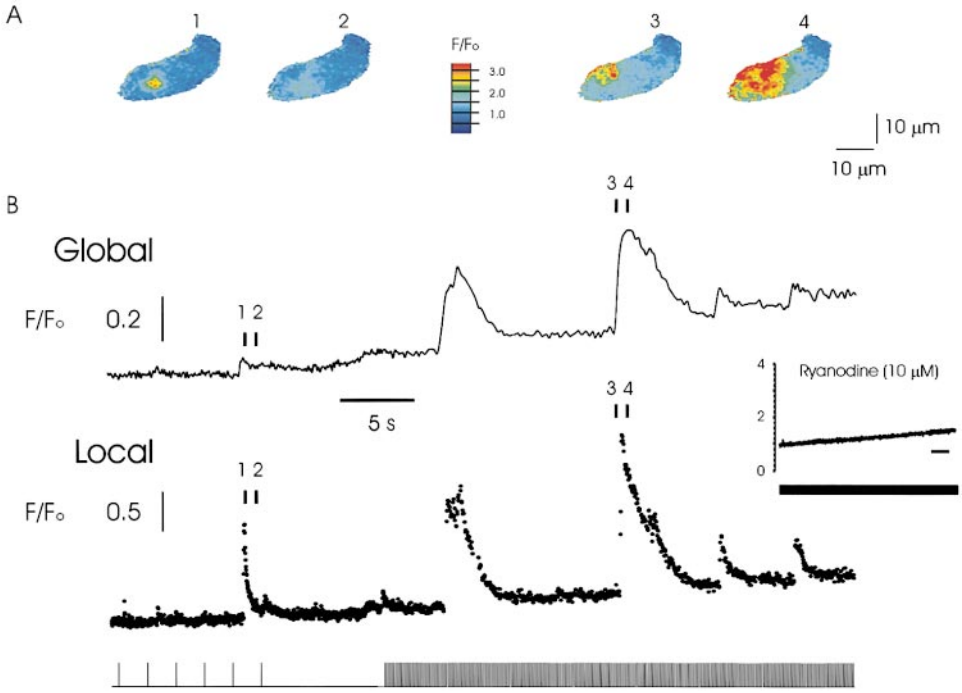

Figure 6. Calcium-induced calcium release is loosely coupled to depolarizing stimuli. Low frequency depolarizing stimuli do not produce calcium release with every depolarization. Rather, a sufficient number of low frequency depolarizations result in nonpropagated Ca^{2+} sparks (local signal), and higher frequency stimuli produce repeated Ca^{2+} sparks that are propagated as Ca^{2+} waves (local and global signals). (A) Confocal x–y images of a smooth muscle cell during depolarizing stimuli applied at 2 s, and then at 0.1-s intervals. Images were obtained at the positions indicated below. (B) Profiles from images as above obtained every 16.7 ms. The global signal (above) shows the average relative fluorescence of the entire cell, and the local signal is from a 10 × 10 pixel region at the point of Ca^{2+} spark initiation. The inset shows the absence of Ca^{2+} sparks in a cell stimulated at 0.1-s intervals, after exposure to 10 µM ryanodine.

meating Ca^{2+} ions within the microdomain of a single L-type Ca^{2+} channel, such that opening of a single L-type Ca^{2+} channel is sufficient to activate a Ca^{2+} spark, since: (a) the occurrence of Ca^{2+} sparks is stochastic with a voltage sensitivity equivalent to the gating behavior of the L-type Ca^{2+} channel (Cannell et al., 1995; Collier et al., 1999); (b) the latency to occurrence of a Ca^{2+} spark after depolarization is equivalent to the latency to opening of an individual L-type Ca^{2+} channel (Lopez-Lopez et al., 1995; Santana et al., 1996; Collier et al., 1999); and (c) the coupling process is not disrupted in the presence of high concentrations of mobile Ca^{2+} buffer (Collier and Berlin, 1999).

Despite the broad expression of L-type Ca^{2+} channels and RYR in many cell types, the existence and nature of CICR in nonsarcomeric cells, in which the distribution of L-type Ca^{2+} channels and RYR differs substantially from an orderly dyadic pattern, is not well established. In smooth muscle, evidence for CICR has been inferred from caffeine- and ryanodine-sensitive Ca_i transients evoked upon I_{Ca} activation (Zholos et al., 1992; Ganitkevich and Isenberg, 1992, 1995). More recently, confocal line-scan images acquired during flash photolysis of caged Ca^{2+} or peak I_{Ca} activation gave rise to localized increases in Ca^{2+} (Arnaudeau et al., 1997) and 2-D confocal images acquired during step depolarizations demonstrated areas of increased fluorescence intensity or "hot spots" (Imaizumi et al., 1998). Direct examination of CICR and the mechanism underlying the coupling between L-type Ca^{2+} channels and RyR is lacking, however.

Using both 2-D and line-scan confocal modes, we examined CICR as a function of the amplitude and duration of I_{Ca}, and provide direct visualization of CICR in x–y images obtained every 8.3 ms. A prominent feature of Ca^{2+} sparks activated by I_{Ca} is the very low number of evoked Ca^{2+} sparks relative to that seen during depolarization of cardiac myocytes (Figs. 1 and 2). While the frequency of Ca^{2+} sparks may be a function of SR loading and modulatory factors (Porter et al., 1998), the number of sparks observed after activation of I_{Ca} is dramatically lower than observed in cardiac cells and the ability to evoke Ca^{2+} release and Ca^{2+} waves with caffeine application suggests that the low efficiency of CICR coupling cannot be explained by poorly loaded SR. Visualization of individual Ca^{2+} sparks in heart cells requires that the amplitude of I_{Ca} be reduced (Cannell et al., 1995; Lopez-Lopez et al., 1995), while they were readily observed in bladder myocytes during voltage-clamp steps to activate I_{Ca}. Moreover, in smooth muscle, individual Ca^{2+} sparks spread in the form of a propagated Ca^{2+} wave, whereas in cardiac myocytes depolarization appears to result in CICR from each dyad, with little required propagation. Our data indicate that both the initial Ca^{2+} spark and the subsequent propagation occurs through the gating of RYR, since both were eliminated in the presence of ryanodine, and neither were affected by dialysis with heparin (Fig. 1).

A second major feature of CICR in smooth muscle relates to the nature of the coupling between the channels. Rather than every opening of L-type Ca^{2+} channels activating a Ca^{2+} spark, Ca^{2+} spark activation in smooth muscle cells was only observed when I_{Ca} was of sufficient magnitude or duration (Figs. 2 and 3). We term this relationship "loose coupling" since it differs dramatically from the obligate tight coupling that exists in heart cells. From experiments such as that shown in Figs. 2 and 3, it is clear that the opening of hundreds of L-type Ca^{2+} channels may not be sufficient to activate a Ca^{2+} spark if channel openings are not of sufficient duration. Experiments specifically designed to maximize single-channel amplitude and open-state probability, but minimize calcium flux, indicated that brief channel openings of maximal amplitude failed to activate Ca^{2+} sparks, whereas increasing the net Ca^{2+} flux at a lower single channel amplitude activated CICR. Thus, in smooth muscle, sufficient aggregate L-type Ca^{2+} channel activity is required to produce CICR in the form of discrete Ca^{2+} sparks, and further Ca^{2+} flux and increased global $[Ca^{2+}]_i$ produces CICR in the form of propagated Ca^{2+} waves (Figs. 2 add 3). Taken together, these data indicate that RYRs appear to be coupled to L-type Ca^{2+} channels through a rise in global $[Ca^{2+}]_i$, rather than local elevations near the channel. This finding was further supported by the disruption of coupling by high concentrations of mobile Ca^{2+} buffer, conditions that do not affect the coupling between L-type Ca^{2+} channels and RYR in cardiac myocytes (Fig. 5). While these data could be explained by an increase in the spacing distance between the sarcolemmal and sarcoplasmic reticulum Ca^{2+} channels (L-type and RYR), it is also possible that the relatively few sites at which Ca^{2+} sparks are repeatedly observed (Imaizumi et al., 1998; Gordienko et al., 1998) represent a concentration of RYR sufficient to generate a resolvable Ca^{2+} spark, and that close connections exist between L-type Ca^{2+} channels and individual RYR, as has been reported (Carrington et al., 1995), but that these do not occur in the density required to generate a resolvable Ca^{2+} spark.

What then is the likely physiological relevance of loose coupling? In skeletal and cardiac myocytes, each action potential results in a twitch response that derives from RYR-mediated calcium release, triggered by local signals in the microdomain of the L-type Ca^{2+} channels. Thus, every neural signal evoking a postsynaptic action potential is obligatorily linked to a mechanical response. Moreover, in addition to tight coupling, the signal gain is quite high, since each channel opening results in a Ca^{2+} spark (activation of several RYRs), the duration of which is longer than the L-type Ca^{2+} channel opening (Cannell et al., 1995). We show here that in

smooth muscle each action potential is not necessarily linked to CICR (Fig. 6), due to a coupling process that requires a sufficient rise in global $[Ca^{2+}]_i$. The uncoupling of Ca^{2+} release from the action potential introduces signal processing elements into the contractile response of smooth muscle. Features of "loose coupling" system are low gain (multiple L-type Ca^{2+} channels must open to produce Ca^{2+} sparks), discriminated responses (release takes the form of local Ca^{2+} sparks or globally propagated Ca^{2+} waves), and a marked lengthening of signal duration (Ca^{2+} waves last far longer than the action potential). Slight variations in this low gain, integrating system, such as a decrease in L-type Ca^{2+} channel density, likely underlies the fact that I_{Ca} does not appear to produce appreciable Ca^{2+} release in some smooth muscle cells, despite the presence of functional RYRs (Fleischmann et al., 1996; Kamishima and McCarron, 1996). The dependence of Ca^{2+} release during E-C coupling on global increases in $[Ca^{2+}]_i$ contrasts with the local signaling that underlies relaxation mediated by spontaneous Ca^{2+} release and the activation of sarcolemmal potassium channels (Nelson et al., 1995), providing a further example of a way in which local and global $[Ca^{2+}]_i$ signals can be exploited to provide flexible cellular responses (Berridge, 1997).

In summary, in the present study, we provide direct evidence of RYR-mediated Ca^{2+} release evoked by the L-type calcium current (CICR) in smooth muscle, demonstrate that the trigger stimulus for the Ca^{2+} release process is a global rather than local rise in $[Ca^{2+}]_i$, and show that this results in a functional uncoupling of a single action potential from Ca^{2+} release in smooth muscle cells. "Loose coupling" between L-type Ca^{2+} channels and RYR allows a functional uncoupling of the action potential and calcium release and provides a mechanism by which neural signals encoded at higher frequencies are transferred to slower mechanical responses.

We thank Drs. Clara Franzini-Armstrong, W.K. Chandler, and Joshua R. Berlin for helpful comments, and Mr. Mario Brenes for technical support.

Supported by National Institutes of Health (NIH) grants HL45239 and DK52620 (to M.I. Kotlikoff). M.L. Collier is a NIH postdoctoral fellow (T32-DK07708-06).

Submitted: 30 August 1999
Revised: 28 March 2000
Accepted: 28 March 2000

REFERENCES

Armstrong, C.M., F.M. Bezanilla, and P. Horowicz. 1972. Twitches in the presence of ethylene glycol bis(-aminoethyl ether)- *N*,*N*′-tetracetic acid. *Biochim. Biophys. Acta.* 267:605–608.

Arnaudeau, S., F.X. Boittin, N. Macrez, J.L. Lavie, C. Mironneau, and J. Mironneau. 1997. L-type and Ca^{2+} release channel-dependent hierarchical Ca^{2+} signalling in rat portal vein myocytes. *Cell Calc.* 22:399–411.

Berridge, M.J. 1997. Elementary and global aspects of calcium signalling. *J. Exp. Biol.* 200:315–319.

Bezprozvanny, I. 1994. Theoretical analysis of calcium wave propagation based on inositol (1,4,5)-trisphosphate (InsP3) receptor functional properties. *Cell Calc.* 16:151–166.

Cannell, M.B., H. Cheng, and W.J. Lederer. 1995. The control of calcium release in heart muscle. *Science.* 268:1045–1049.

Carrington, W.A., R.M. Lynch, E.D. Moore, G. Isenberg, K.E. Fogarty, and F.S. Fay. 1995. Superresolution three-dimensional images of fluorescence in cells with minimal light exposure. *Science.* 268:1483–1487.

Cheng, H., W.J. Lederer, and M.B. Cannell. 1993. Calcium sparks: elementary events underlying excitation–contraction coupling in heart muscle. *Science.* 262:740–744.

Collier, M.L., and J.R. Berlin. 1999. Sarcoplasmic reticulum Ca^{2+} release is activated by localized Ca^{2+} influx during cardiac excitation–contraction coupling. *Biophys. J.* 76:A463. (Abstr.)

Collier, M.L., A.P. Thomas, and J.R. Berlin. 1999. Relationship between L-type Ca^{2+} current and unitary sarcoplasmic reticulum Ca^{2+} release events in rat ventricular myocytes. *J. Physiol.* 516: 117–128.

Endo, M. 1977. Calcium release from the sarcoplasmic reticulum. *Physiol. Rev.* 57:71–108.

Fabiato, A. 1983. Calcium-induced release of calcium from the cardiac sarcoplasmic reticulum. *Am. J. Physiol. Cell Physiol.* 245:C1–C14.

Fabiato, A. 1985. Simulated calcium current can both cause calcium loading in and trigger calcium release from the sarcoplasmic reticulum of a skinned canine cardiac Purkinje cell. *J. Gen. Physiol.* 85:291–320.

Fleischmann, B.K., Y.X. Wang, M. Pring, and M.I. Kotlikoff. 1996. Voltage-dependent calcium currents and cytosolic calcium in equine airway myocytes. *J. Physiol.* 492:347–358.

Ganitkevich, V.Y., and G. Isenberg. 1995. Efficacy of peak Ca^{2+} currents (I_{Ca}) as trigger of sarcoplasmic reticulum Ca^{2+} release in myocytes from the guinea-pig coronary artery. *J. Physiol.* 484:287–306.

Ganitkevich, V.Y., and G. Isenberg. 1992. Contribution of Ca^{2+}-induced Ca^{2+} release to the $[Ca^{2+}]_i$ transients in myocytes from guinea-pig urinary bladder. *J. Physiol.* 458:119–137.

Gordienko, D.V., T.B. Bolton, and M.B. Cannell. 1998. Variability in spontaneous subcellular calcium release in guinea-pig ileum smooth muscle cells. *J. Physiol.* 507:707–720.

Imaizumi, Y., Y. Torii, Y. Ohi, N. Nagano, K. Atsuki, H. Yamamura, K. Muraki, M. Watanabe, and T.B. Bolton. 1998. Ca^{2+} images and K^+ current during depolarization in smooth muscle cells of the guinea-pig vas deferens and urinary bladder. *J. Physiol.* 510:705–719.

Kamishima, T., and J.G. McCarron. 1996. Depolarization-evoked increases in cytosolic calcium concentration in isolated smooth muscle cells of rat portal vein. *J. Physiol.* 492:61–74.

Klingauf, J. and E. Neher. 1997. Modeling buffered Ca^{2+} diffusion near the membrane: implications for secretion in neuroendocrine cells. *Biophys. J.* 72:674–690.

Klockner, U., and G. Isenberg. 1985. Calcium currents of cesium loaded isolated smooth muscle cells (urinary bladder of the guinea-pig). *Pflügers Arch.* 405:340–348.

Lesh, R.E., G.F. Nixon, S. Fleischer, J.A. Airey, A.P. Somlyo, and A.V. Somlyo. 1998. Localization of ryanodine receptors in smooth muscle. *Circ. Res.* 82:175–185.

Lipp, P., and E. Niggli. 1996. Submicroscopic calcium signals as fundamental events of excitation–contraction coupling in guinea-pig cardiac myocytes. *J. Physiol.* 492:31–38.

Lopez-Lopez, J.R., P.S. Shacklock, C.W. Balke, and W.G. Wier. 1995.

Local calcium transients triggered by single L-type calcium channel currents in cardiac cells. *Science.* 268:1042–1045.

McPherson, P.S., and K.P. Campbell. 1993. The ryanodine receptor/Ca^{2+} release channel. *J. Biol. Chem.* 268:13765–13768.

Mironneau, J., S. Arnaudeau, N. Macrez-Lepretre, and F.X. Boittin. 1996. Ca^{2+} sparks and Ca^{2+} waves activate different Ca^{2+}-dependent ion channels in single myocytes from rat portal vein. *Cell Calc.* 20:153–160.

Nabauer, M., G. Callewaert, L. Cleemann, and M. Morad. 1989. Regulation of calcium release is gated by calcium current, not gating charge, in cardiac myocytes. *Science.* 244:800–803.

Nakai, J., T. Tanabe, T. Konno, B. Adams, and K.G. Beam. 1998. Localization in the II–III loop of the dihydropyridine receptor of a sequence critical for excitation–contraction coupling. *J. Biol. Chem.* 273:24983–24986.

Nelson, M.T., H. Cheng, M. Rubart, L.F. Santana, A.D. Bonev, H.J. Knot, and W.J. Lederer. 1995. Relaxation of arterial smooth muscle by calcium sparks. *Science.* 270:633–637.

Niggli, E. and W.J. Lederer. 1990. Real-time confocal microscopy and calcium measurements in heart muscle cells: towards the development of a fluorescence microscope with high temporal and spatial resolution. *Cell Calc.* 11:121–130.

Perez, G.J., A.D. Bonev, J.B. Patlak, and M.T. Nelson. 1999. Functional coupling of ryanodine receptors to K_{Ca} channels in smooth muscle cells from rat cerebral arteries. *J. Gen. Physiol.* 113:229–238.

Porter, V.A., A.D. Bonev, H.J. Knot, T.J. Heppner, A.S. Stevenson, T. Kleppisch, W.J. Lederer, and M.T. Nelson. 1998. Frequency modulation of Ca^{2+} sparks is involved in regulation of arterial diameter by cyclic nucleotides. *Am. J. Physiol. Cell Physiol.* 274:C1346–C1355.

Rubart, M., J.B. Patlak, and M.T. Nelson. 1996. Ca^{2+} currents in cerebral artery smooth muscle cells of rat at physiological Ca^{2+} concentrations. *J. Gen. Physiol.* 107:459–472.

Santana, L.F., H. Cheng, A.M. Gomez, M.B. Cannell, and W.J. Lederer. 1996. Relation between the sarcolemmal Ca^{2+} current and Ca^{2+} sparks and local control theories for cardiac excitation–contraction coupling. *Circ. Res.* 78:166–171.

Tanabe, T., K.G. Beam, B.A. Adams, T. Niidome, and S. Numa. 1990. Regions of the skeletal muscle dihydropyridine receptor critical for excitation–contraction coupling. *Nature.* 346:567–569.

Wang, Y.-X., and M.I. Kotlikoff. 1997. Inactivation of calcium-activated chloride channels in smooth muscle by calcium/calmodulin dependent protein kinase. *Proc. Natl. Acad. Sci. USA.* 94: 14918–14923.

Wier, W.G., T.M. Egan, J.R. Lopez-Lopez, and C.W. Balke. 1994. Local control of excitation–contraction coupling in rat heart cells. *J. Physiol.* 474:463–471.

Wussling, M.H., K. Scheufler, S. Schmerling, and V. Drygalla. 1997. Velocity–curvature relationship of colliding spherical calcium waves in rat cardiac myocytes. *Biophys. J.* 73:1232–1242.

Zholos, A.V., L.V. Baidan, and M.F. Shuba. 1992. Some properties of Ca^{2+}-induced Ca^{2+} release mechanism in single visceral smooth muscle cell of the guinea-pig. *J. Physiol.* 457:1–25.